The Evolution of the Plateau, an Optical Coherence Tomography Signature Seen in Geographic Atrophy

Anna C. S. Tan,[1–3] Polina Astroz,[1,4] Kunal K. Dansingani,[1,2,5] Jason S. Slakter,[1] Lawrence A. Yannuzzi,[1,2] Christine A. Curcio,[6] and K. Bailey Freund[1,2,7]

[1]Vitreous Retina Macula Consultants of New York, New York, New York, United States
[2]The LuEsther T. Mertz Retinal Research Center, New York, New York, United States
[3]Singapore National Eye Center/Singapore Eye Research Institute/Duke-NUS Medical School, Singapore, Singapore
[4]Department of Ophthalmology, Intercity Hospital and University Paris Est, Creteil, France
[5]Truhlsen Eye Institute, University of Nebraska Medical Center, Omaha, Nebraska, United States
[6]Department of Ophthalmology, University of Alabama School of Medicine, Birmingham, Alabama, United States
[7]Department of Ophthalmology, New York University School of Medicine, New York, New York, United States

PURPOSE. Histologic details of progression routes to geographic atrophy (GA) in AMD are becoming available through optical coherence tomography (OCT). We studied the origins and evolution of an OCT signature called plateau in eyes with GA and suggested a histologic correlate.

METHODS. Serial eye-tracked OCT scans and multimodal imaging were acquired from eight eyes of seven patients with GA and plateau signatures over a mean follow-up of 7.7 years (range, 3.7–11.6). The histology of unrelated donor eyes with AMD was reviewed.

RESULTS. Drusenoid pigment epithelial detachment (PED) on OCT imaging progressed into wide-based mound-like signatures with flattened apices characterized by a hyporeflective yet heterogeneous interior and an overlying hyperreflective exterior, similar to outer retinal corrugations previously ascribed to persistent basal laminar deposit (BLamD) but larger. These new signatures are described as "plateaus." An initial increase of the PED volume and hyporeflectivity of its contents was followed by a decrease in PED volume and thinning of an overlying hyperreflective band attributable to the loss of the overlying RPE leaving persistent BLamD. Both imaging and histology revealed persistent BLamD with defects through which gliotic Müller cell processes pass.

CONCLUSIONS. Plateaus can be traced back to drusenoid PEDs on OCT imaging. We hypothesize that during progressive RPE atrophy, Müller cell extension through focal defects in the residual persistent BLamD may contribute to the heterogeneous internal reflectivity of these entities. The role of Müller cell activation and extension in the pathogenesis of AMD should be explored in future studies.

Keywords: drusenoid pigment epithelial detachment, geographic atrophy, histology, multimodal imaging, optical coherence tomography

Advanced AMD is a significant cause of central vision loss in the elderly population[1,2] and, although treatment options currently exist for neovascular AMD,[3] no evidence-based therapy is yet effective in treating or preventing atrophic AMD, also known as geographic atrophy (GA).[4,5] Advances in multimodal imaging technology, including fundus autofluorescence (FAF) and optical coherence tomography (OCT), have allowed detailed in vivo study of early AMD features and identification of high-risk features associated with the progression of drusen and drusenoid pigment epithelial detachments (PEDs) into GA.[6–8] In addition, the retrospective use of serial eye-tracked OCT imaging allows the study of the origins and evolution of end-stage features seen within GA areas, providing valuable insights into disease pathogenesis.[9] Recently, we described a characteristic growth and collapse of large PEDs in which collapse was preceded by a roughening of the RPE–Bruch's membrane (BrM) band followed by the appearance directly above, within the retina, of hyperreflective foci believed to be RPE.[10] Growth and collapse is common to drusen of all sizes, and presence of hyperreflective foci over drusen can predict progression, so these RPE changes before atrophy may be generalizable.[11,12]

OCT imaging has revealed various distinctive signatures, both within the atrophic area and around the GA margin, some of which, including outer retinal tubulation (ORT)[13] and outer retinal corrugation,[14] have been assigned histologic correlates. In particular, outer retinal corrugation could be correlated with persistence of basal laminar deposit (BLamD). BLamD is a stereotypically structured thick layer of basement membrane material with other components that is interposed between the RPE plasma membrane and the original basal lamina. BLamD is hyporeflective when the RPE is present and hyperreflective when the RPE is not present.[14] Other OCT signatures, such as "hyperreflective crown-like structures," "hyperreflective pyramidal structures" (HPS), and "ghost drusen,"[13–16] do not yet have agreed-on correlates. By seeking histologic correlates, we can fill in gaps in the progression sequence and gain an accurate picture of the timing and spatial characteristics of RPE
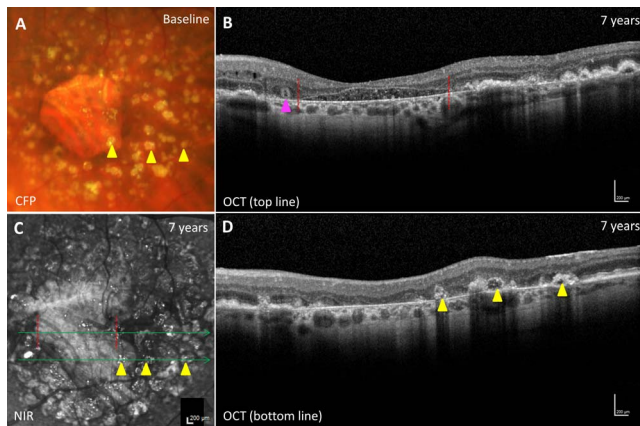
FIGURE 1. Multimodal imaging shows differences between the appearance of the plateau, refractile drusen and HPS. CFP (**A**) taken at baseline, follow-up NIR (**C**), and OCT images (**B**, **D**) taken 7 years later. *Green lines* (**C**) show corresponding cross-sectional OCT images (**B**, *top green arrow*; **D**, *bottom green arrow*). Boundaries of the plateau base are well demarcated on OCT but appear isoreflective on NIR (**B**, **C**, *red dotted lines*). Other structures that are distinct from the plateau include a closed outer retinal tubulation (*pink arrowhead*) and HPS (**D**, *yellow arrowheads*) that appear as refractile drusen on CFP and hyperreflective on NIR (**A**, **C**, *yellow arrowheads*). Some HPS contain a hyporeflective core surrounded by hyperreflective dots.

atrophy over drusen and PEDs. In turn, an accurate and comprehensive timeline can prompt new mechanistic hypotheses of cell death that are experimentally testable in model systems, leading to new therapeutic strategies.

Recently, Querques et al.[17] described an uncommon "wedge-shaped subretinal hyporeflectivity" within areas of atrophy delimited externally by the hyperreflective bands representing BrM and internally by the synaptic portion of the outer plexiform layer (OPL). It should be noted that this description differed markedly from the common "hyporeflective wedge-shaped band" described by Monés et al.,[18] which develops in the axonal portion of the OPL (Henle fiber layer) at the junction between normal and atrophic retina.[6,19] The descriptor "hyporeflective wedge" applied to two different structures in GA has caused some confusion in recent literature.[19,20] Histologic correlates have not been proposed for either of these OCT signatures.

The purpose of our study was to examine the origins and evolution of the Querques' "wedge-shaped subretinal hyporeflectivity"[17] using serial eye-tracked OCT imaging and to propose a histologic correlate. The term "wedge" suggested to us a triangle-shaped structure. After studying many such lesions in detail, we observed that most are not triangular but instead are mound-like with a flattened apex and a wide base, resembling a "plateau" (Fig. 1). Based on these observations, and to avoid further confusion in terminology, we propose "plateau" (plural plateaus or plateaux) as a more accurate descriptor than "wedge." Of note, plateaus should be differentiated from other tomographic signatures seen in eyes with GA such as ORT, refractile drusen, and HPS (Fig. 1).[15,16,21] We find that plateau natural history can be differentiated from that described for PED collapse, thus providing a basis for considering outer retinal corrugations and plateaus a continuum of OCT signatures involving persistent BLamD.

METHODS

This retrospective observational study was approved by the Western Institutional Review Board (Olympia, Washington,

USA). It complied with the Health Insurance Portability and Accountability Act of 1996 and followed the tenets of the Declaration of Helsinki. Informed consent was obtained from the subjects after explanation of the nature and possible consequences of the study.

Study Cohort

Patients with GA were identified from the tertiary practice of retinal specialists (KBF, JS, and LY) if they exhibited plateau signatures in at least one eye (study eye) on OCT imaging and if they also had at least 3 years' follow-up with consecutive eye-tracked spectral-domain (SD)-OCT scans taken at least every 6 months. Eyes with macular neovascularization, other retinal pathology, or media opacity preventing adequate imaging were excluded.

Imaging Protocol and Analysis

Medical records and multimodal imaging, including color fundus photography (CFP), red-free photography (RF), fundus autofluorescence (FAF), near-infrared reflectance scanning laser ophthalmoscopy (NIR), and SD-OCT was performed on all the patients. CFP and RF were performed with a TRC-50IX flood-illuminated fundus camera (Topcon Medical Systems, Oakland, NJ, USA). FAF was performed with either the Spectralis HRA + OCT (Heidelberg Engineering, Heidelberg, Germany) or the Topcon TRC-50IX fundus camera. SD-OCT imaging with corresponding NIR images was performed on the Spectralis. OCT scans taken before the acquisition of eye-tracked Spectralis scans were assessed qualitatively but not included in the quantitative analysis. The SD-OCT protocol used in all eyes comprised 20° horizontal raster line scans over the area of interest, ranging from 19 to 49 B-scans per eye, with each scan spaced 115 to 250 μm apart, and automatic real-time averaging set between 4 and 23.

To study the origin and progression of plateaus, the most recent SD-OCT with this signature was identified. Then, serial eye-tracked B-scans of the region of interest were tracked back to baseline. In cases in which the scanning protocol varied during the course of follow-up, the B-scan closest to the area of interest was matched manually and extracted for analysis. These extracted SD-OCT images were then stacked, aligned, and saved as a video file using the Fiji distribution ("Fiji is just Image J," http://fiji.sc; in the public domain)[22] for the qualitative analysis of the progression of the lesion (see Supplementary Video). At each time point, the plateau appearance on SD-OCT was correlated to the appearance in CFP, NIR, and FAF.

Three patients had en face OCT and OCT angiography (OCTA) imaging with 3 × 3-mm macular cubes (RTVue XR "Avanti"; Optovue, Fremont, CA, USA). The review software (ReVUe, Version 2015.1.0.90; Optovue, Fremont, CA, USA) displays flow signals superimposed in red on a cross-sectional structural SD-OCT image.

SD-OCT Terminology

In a healthy eye, the fourth outer retinal hyperreflective band includes the RPE and BrM.[23] In a PED, by definition, the RPE is separated from the BrM. In the course of this separation, either a basal lamina (BL) of 0.15-μm thickness[24] or a BLamD of variable thickness adheres to the RPE and not to the BrM. Therefore, we call the hyperreflective band that anteriorly delimits a PED the RPE-BL complex. The definition of a "plateau" was a distinct OCT signature where a mound-like structure with a flattened apex and a wide base was observed within an area of GA after complete loss of the overlying RPE.
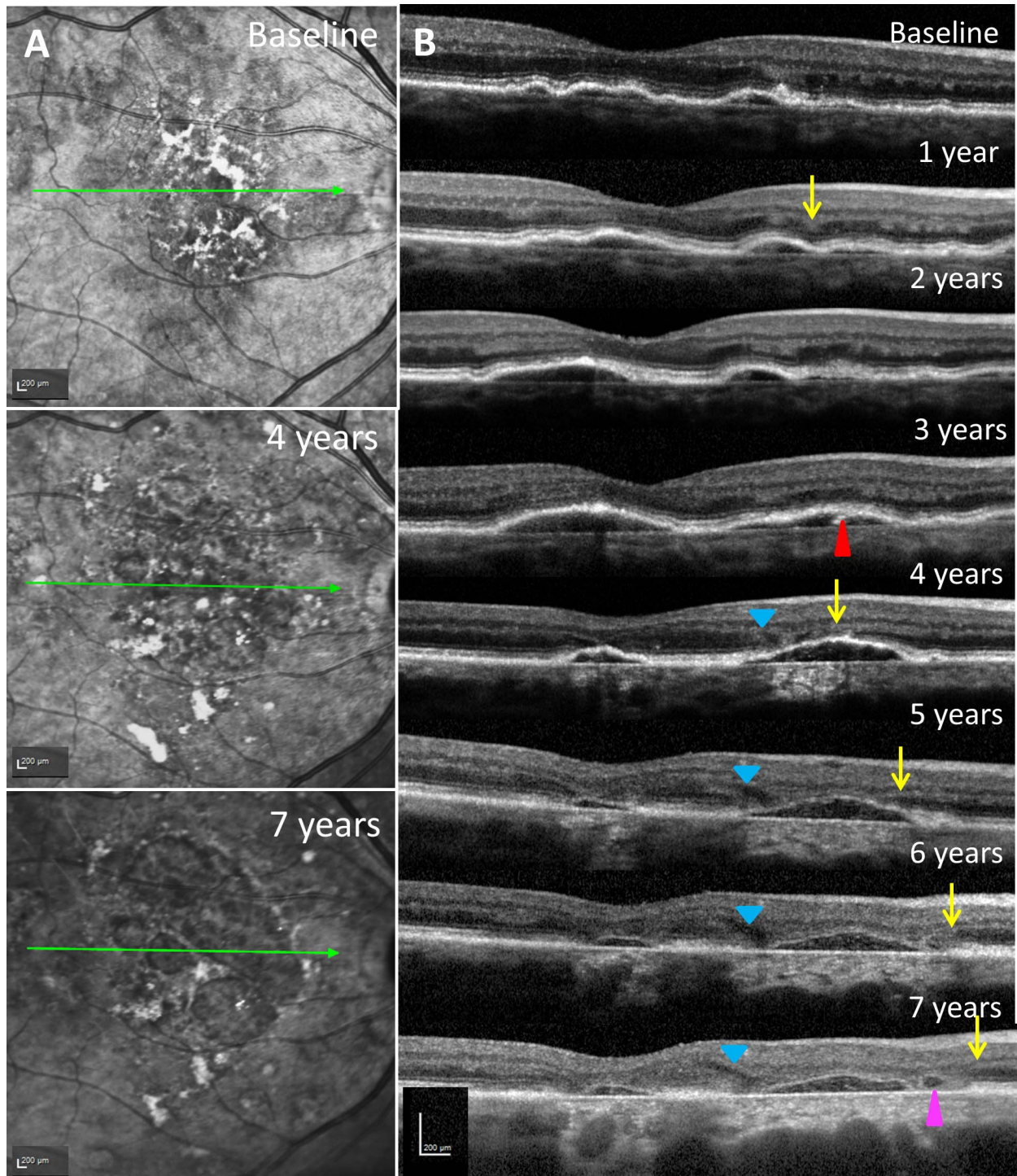
FIGURE 2. Origin and evolution of a plateau, as revealed by NIR (**A**) and OCT (**B**) images. NIR images show progressive GA. *Green arrows* on NIR images show the levels of corresponding OCT cross-sectional images. Baseline images show several elevations of the RPE with largely hyporeflective interiors. At 3 years after baseline, punctate hyperreflectivity (*red arrowhead*) is seen in the sub-RPE compartment. At 4 years, progressive loss of the ONL has caused the OPL (*yellow arrows*) to approach the surface of the PED. Also at 4 years, a "Monés hyperreflective wedge" (*blue arrowheads*) appears at the GA border. At 5 years, the downwardly deflected OPL is seen to move progressively toward the edge of the plateau following the advancing border of GA. Formation of the plateau at 5 years was characterized by the loss of the overlying RPE causing marked thinning of the hyperreflective RPE-basal lamina complex now reduced to just BLamD, compared with at 4 years. At 7 years, a closed ORT (*pink arrowhead*) is present adjacent to the plateau.

Quantification of Volume Changes During Progression

To determine the volume of the drusenoid PED and ensuing plateau (Fig. 2), the Cavalieri principle of stereology was applied to SD-OCT volumetric data acquired at each visit,[10,25,26] as follows. (1) Each B-scan in the volume was scaled to a 1:1 pixel aspect ratio. The caliper function within the Heidelberg Eye Explorer software (version 6.3.4.0; Heidelberg Engineering) was used to measure the area

between the outer boundary of RPE+BL and the inner boundary of BrM. (2) the volume between two consecutive OCT slices (hereafter called a segment) was then determined using the following formula:

$$d((A\_x + A\_(x + 1))/2),$$

where d is the distance between consecutive slices in μm, A is the area between the RPE+BL and BrM in μm^2, and x is the OCT slice number. (3) Total PED volume was calculated by summing the volumes of individual segments. The number of segments in the OCT volume was $(n - 1)$, where n is the total number of slices that spanned the PED. Graphical plots of PED volume with respect to time were generated using interval data.

Histology Study

The institutional review board at University of Alabama at Birmingham (UAB) approved the laboratory study, which complied with the Health Insurance Portability and Accountability Act and adhered to the tenets of the Declaration of Helsinki. AMD eyes were identified through an ex vivo imaging screen of eyes accessioned for research purposes from nondiabetic white donors to the Alabama Eye Bank during the period 1996 to 2012. Median death-to-preservation time was 3:49 hours (range, 0:40–11:40 hours). Thirteen eyes with GA were reviewed for examples suitable for this study. Ophthalmic health records were not available for these donors. Eyes were preserved by immersion in 1% paraformaldehyde and 2.5% glutaraldehyde in 0.1 M phosphate buffer following anterior segment excision. After vitreous removal, maculas were photographed in color on a stereomicroscope (SMZ-U; Nikon, Melville, NY, USA).[27] When prepared for histology (2011–2013) and uploaded to the Project MACULA Web site (http://projectmacula.cis.uab.edu, in the public domain), eyes underwent additional multimodal ex vivo imaging. From each globe, an 8-mm-diameter full-thickness tissue punch containing the fovea and temporal portion of the optic nerve head was held in a tissue holder mounted on a Spectralis, as described.[27] A 30° × 20° SD-OCT volume (143 scans, 30-μm spacing, automated real-time averaging [ART] = 25) was captured along with red-free and near-infrared reflectance scanning laser ophthalmoscopic images. Tissue punches were postfixed by osmium tannic acid paraphenylenediamine to accentuate extracellular lipid and embedded in epoxy resin (PolyBed 812; Polysciences, Warrington, PA, USA).[28] Sub-micrometer-thick (0.8 μm) sections at 25- to 30-μm intervals were stained with 1% toluidine blue for polychromaticity, scanned with a ×40 objective, and reviewed and photodocumented with a ×60 oil-immersion objective (numerical aperture = 1.4) and digital camera (XC10; Olympus, Center Valley, PA, USA). Images were adjusted for exposure, contrast, and sharpness (Photoshop CS6, Adobe, San Jose, CA, USA).

RESULTS

Patient Characteristics

Plateau signatures were observed in eight eyes of seven patients, of whom six were female. Mean age was 75 years (range, 60–89) and mean follow-up period was 7.7 years (range, 3.7–11.6). Baseline visual acuity (VA) was logMAR 0.42 (Snellen equivalent 20/52) (range, 0.18–1). Final VA was logMAR 1.16 (Snellen equivalent 20/289) (range, 0.18–2.3). In two eyes, GA spared the fovea throughout the entire course of the follow-up.

Baseline Features

At baseline, the presence of a drusenoid PED with homogeneous hyperreflective contents and an intact overlying RPE was noted in six eyes (75%; Figs. 2, 3). One eye (patient 5, left eye) had an extremely large PED measuring 2.24 mm^3 with mostly hyporeflective contents and an overlying vitelliform lesion. In another eye (patient 4, left eye), the plateau was already present at baseline. Pigmentary changes noted on CFP were also found on NIR, RF, and FAF in six eyes, and these corresponded to intraretinal hyperreflective foci on OCT (Fig. 3). Overlying the PED surface, the ellipsoid zone and outer nuclear layer (ONL) were thin, with the OPL nearly apposed to the surface of the PED.

Characteristics Seen During Progression of Drusenoid PED into the Plateau

During follow-up, ONL thinning resulted in the OPL approximating the surface of the PED in all cases in which the PED was present at baseline (Figs. 2, 3).[6] As GA progressed, this point of approximation moved toward the edges of the PED base, following the advancing border of GA (Supplementary Video). In all eyes, there was also progressive thinning of the hyperreflective RPE-BL complex and diminution of its reflectivity, beginning at the apex of the PED and advancing toward its edges. This likely represents RPE loss leaving persistent BLamD. After RPE loss occurred over the entire PED surface, the plateau (i.e., a thin hyperreflective inner surface and an interior of heterogeneous and overall reduced reflectivity) appeared.

The plateau surface was highly reflective on both cross-sectional and en face OCT (Fig. 4, en face OCT surface) and showed the presence of focal defects (Fig. 4, yellow arrows). On cross-sectional OCT, the inner contents of the plateau consisted of round, hyporeflective areas (Fig. 4, blue arrows) that were usually accompanied by smaller hyperreflective foci seen beneath the hyperreflective border. These hyperreflective foci also could be observed within the area of GA as hyperautofluorescent foci on FAF and hyperreflective foci on en face OCT (Fig. 4, green arrows). Accordingly, on en face OCT, plateau contents were seen as honeycomb-like structures with hyporeflective spaces interspersed with hyperreflective foci (Fig. 4, en face OCT). The punctate hyperreflective foci (Fig. 4, green arrows) increased in abundance within the plateau interior during follow-up in all eyes as seen on cross-sectional and en face OCT (Figs. 2, 3, 4). On both cross-sectional and en face OCTA, no abnormal flow signals were noted within plateaus (Fig. 4).

Changes in Volume of the Drusenoid PED and Plateau Signature With Time

In seven of eight eyes, the plateau was located in the macula. In one eye, a plateau was located just inferior to the macula at the vascular arcade. A single plateau was seen in all eyes except for one (patient 2) that had two separate plateaus (Fig. 2). Patient 6 had one plateau in each eye. In the seven eyes with a baseline PED, PED volume gradually increased (Fig. 5) due to an increase in the hyporeflective interior. The thinning of the hyperreflective band over the PED surface after RPE loss (at which point we consider the plateau to be formed) was preceded by a sharp decrease in PED volume (Fig. 5). Subsequently, the volume of the residual plateau appeared very stable over time (Fig. 5).

Illustrative Histologic Case

Figure 6 shows histology of a donor eye with GA, for which local relationships and cellular processes in the interior of
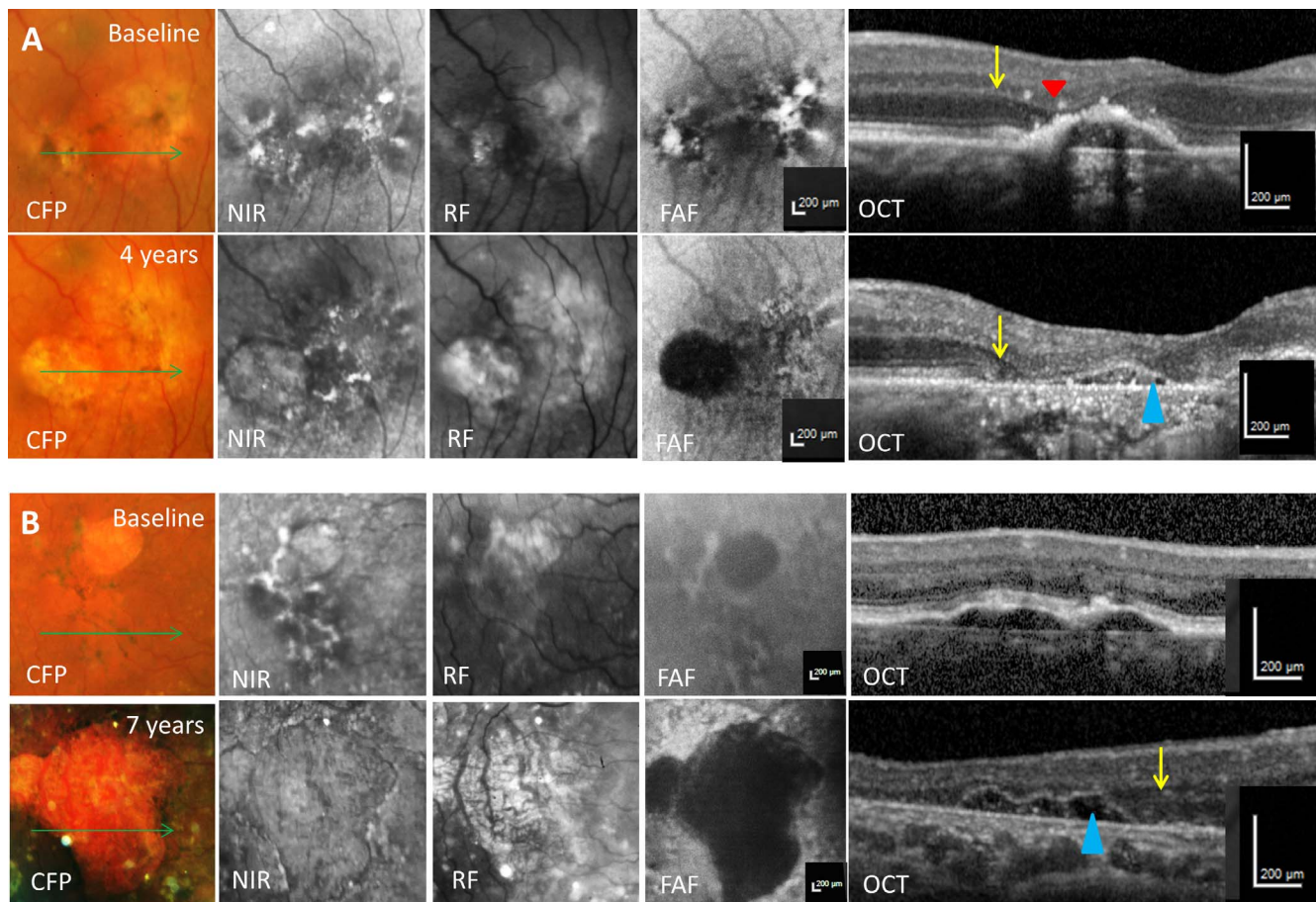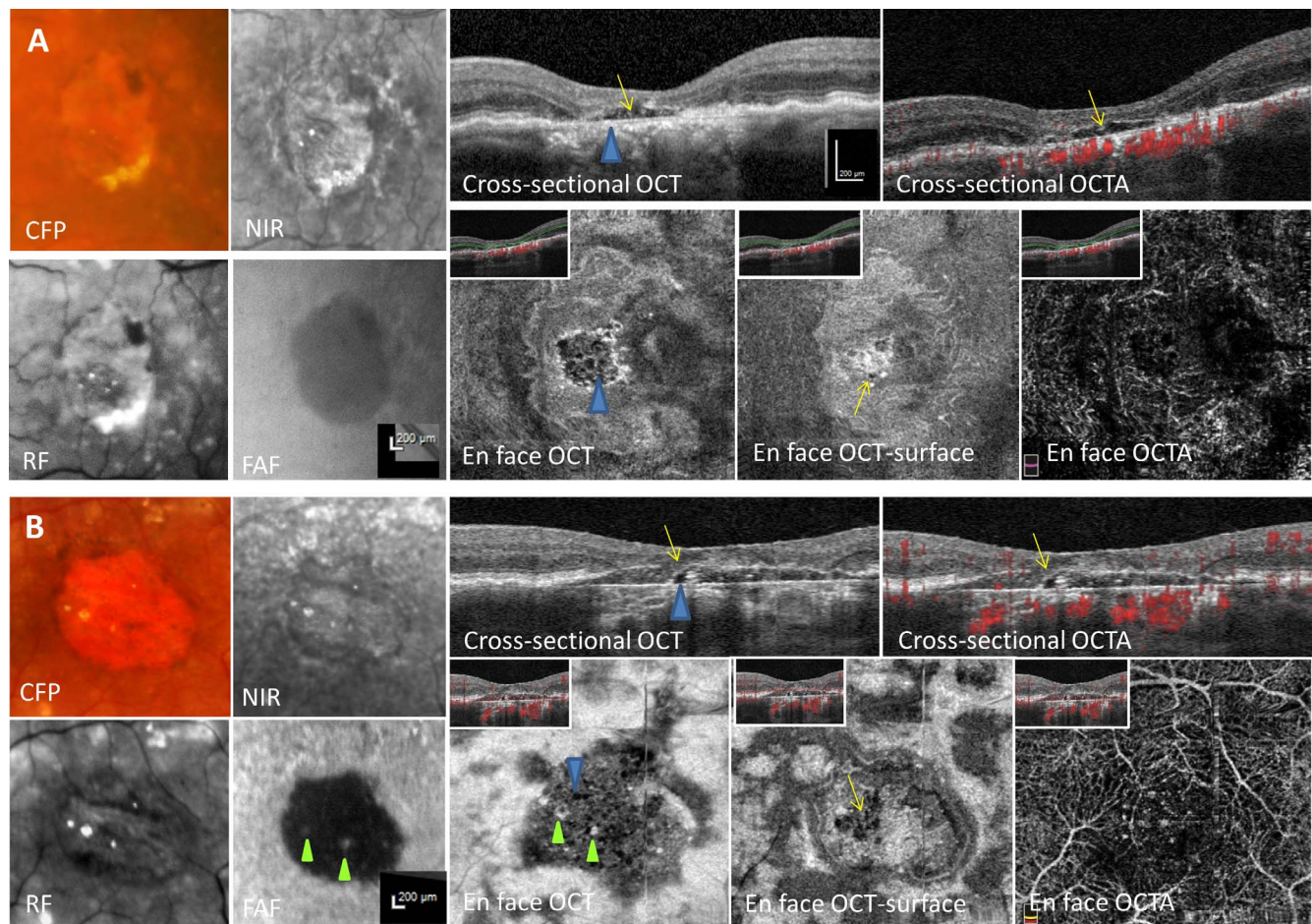
FIGURE 3. Multimodal imaging of two patients (**A**, **B**) at baseline and follow-up (**A**, 4 years; **B**, 7 years). (**A**) At baseline, patient 3 has a drusenoid PED with overlying pigment hyperplasia and hyperautofluorescent vitelliform material. The OCT B-scan shows intraretinal hyperreflective foci (*red arrowhead*) and loss of outer retinal bands over the apex of the PED. The OPL (*yellow arrow*) bends downward toward the PED surface. Four years later, a region of hypoautofluorescent GA contains a plateau that cannot be appreciated in the CFP, NIR, RF, or FAF. The OCT B-scan shows a plateau with a shape similar to the baseline PED. Further loss of ONL has caused the OPL to drape over the plateau. The downwardly deflecting OPL (*yellow arrow*) has moved laterally as it follows the border of the advancing GA. There was marked attenuation and decreased reflectivity of the RPE-BL band. Hyporeflective areas (**A**, *blue arrowhead*) are visible within the plateau interior. (**B**) At baseline, patient 6 has a drusenoid PED with overlying pigment hyperplasia that is located inferior to an area of GA. The OCT B-scan shows a bilobed drusenoid PED. *Bottom row*: Seven years later, the GA has markedly enlarged, and the PED is no longer visible on CFP, NIR, RF, or FAF. The OCT B-scan shows that following progressive loss of the ONL, the OPL (*yellow arrow*) appears draped over a plateau with a shape similar to the baseline PED. There was marked attenuation and decreased reflectivity of the RPE-BL band. Hyporeflective areas (*blue arrowhead*) are visible within the plateau interior.

outer retinal corrugations were particularly clear yet also representative of other GA eyes available for review. Atrophy spared the fovea in this eye, as seen with ex vivo CFP and 488-nm autofluorescence, and small reflective puncta in the atrophic area were apparent on NIR (Figs. 6A–C). In a panoramic view (Fig. 6E), BLamD was seen as discontinuous, being present at three separate locations. Pigmented cells were of the "subducted" phenotype,[29] that is, RPE-originated cells located external to BLamD, in contact with BrM. For reference, in the Henle fiber layer of a normal eye, obliquely oriented Müller cell processes are parallel to, and interleaved with, inner fibers of cone and rod photoreceptors.[30,31] In the presence of severe photoreceptor degeneration, including ORT in this GA eye, the trajectories of gliotic Müller cell processes were oriented in many directions, as indicated by arrows in Figure 6E. In one instance, processes seemed to enter an outer retinal corrugation horizontally through an opening in the BLamD and sweep the "subducted" cells off BrM (Fig. 6D).

DISCUSSION

Through a retrospective review of AMD patients with long-term serial eye-tracked SD-OCT, we identified a series of eyes in which drusenoid PEDs progressed into plateau signatures within areas of GA. Plateaus were seen on OCT to contain heterogeneous reflectivity enclosed by a thin overlying hyper-reflective surface. A focal defect in the hyperreflective surface, in addition to intraretinal and sub-RPE hyperreflective dots, was observed during the evolution of PED into plateau signatures. OPL subsidence was noted to begin at the surface of the PED and progress toward the edge following the areas of expanding atrophy. There was a gradual increase in volume due to an increase in hyporeflective contents initially, followed by complete loss of the RPE and a sharp decrease in PED volume, at which time the plateau was considered to have formed.

The study of drusen life cycles and PED evolution are important to improve our understanding of the pathogenesis of

FIGURE 4. Multimodal imaging of two patients (**A**, **B**). (**A**) A plateau located within the area of GA features internal hyporeflective areas on cross-sectional OCT (*blue arrowhead*), which appear to be organized in a honeycomb-like pattern on en face OCT (*blue arrowhead*). On cross-sectional OCT, OCTA, and on OCT surface (an en face OCT slab at the level of the RPE-BL atop the plateau), the plateau interior is bounded by a distinct hyperreflective band that continues as a thick and highly reflective RPE band. This hyperreflective surface shows transient hyporeflective defects (*yellow arrows*) during the evolution of these lesions. An en face OCT image of the plateau surface allows better appreciation of the focal defects (*yellow arrow*). OCTA does not show flow within the plateau. (**B**) A plateau located within the area of GA features internal hyporeflective areas on cross-sectional OCT (*blue arrowhead*), which appear to be organized in a honeycomb-like pattern on en face OCT (*blue arrowhead*). On cross-sectional OCT and OCTA, a distinct hyperreflective surface surrounds the plateau interior and focal defects (*yellow arrows*) can be seen in some areas. An en face OCT taken at the plateau surface allows better appreciation of focal defects in this hyperreflective layer (en face OCTA: *surface yellow arrow*). Deep to these focal defects are hyperreflective features (FAF and en face OCT: *green arrowheads*) that are also seen on FAF as punctate hyperfluorescence within the confluent area of hypoautofluorescence. OCTA does not show flow within the plateau.

AMD. Understanding the origins and evolution of various OCT findings and correlating these findings to histology enable the in vivo study of microscopic cellular changes occurring in these eyes with progressive GA.[32–34] The development of GA has been previously reported to occur in 19% of eyes with drusenoid PEDs and to be associated with specific features such as subsidence of the OPL and inner nuclear layer and the development of a hyporeflective "wedge-shaped band" within the Henle fiber layer described by Monés et al.[18,20] Half of our study eyes exhibited this wedge. The appearance of plateaus should be distinguished from other signatures previously described in GA, such as ORT, ghost drusen, hyperreflective crown-like structures, HPS, and refractile drusen (Figs. 1, 2).[15,16,21] Plateau boundaries are difficult to distinguish from the surrounding atrophy using CFP, NIR, RF, and FAF (Figs. 1, 3, 4, 6). Previous studies have reported focal areas of hyper-autofluorescence within GA,[17] and in our study these correlated with hyperreflective foci seen on en face OCT (Fig. 4). The presence of many pigmented cells of apparent RPE origin within atrophic areas is now well-documented[35,36]

(Fig. 6), and such cells could give rise to both autofluorescence and OCT hyperreflectivity signals. Plateaus do not contain the highly refractile material as seen on CFP and NIR in eyes with spherules in calcifying drusen.[21] These refractile drusen instead appear to correlate with HPS seen on OCT (Fig. 1), the composition of which is the focus of our ongoing studies.[14] However, both the plateau signatures and HPS (Fig. 1) have a similar overlying thin hyperreflective layer consistent with an overlying BLamD drape, as previously observed in OCT[14] and in histology (Fig. 26 of Sarks et al.,[34] and Fig. 3B of Balaratnasingam et al.[37]).

Our current data support a previous study that suggested that plateaus occur at a low frequency in eyes with GA (7.5%).[17] The plateau is a signature of a residual structure seen on OCT once the RPE has progressed into complete atrophy. In our study, after plateau formation as defined by loss of the overlying RPE layer exposing the underlying BLamD that then persists, minimal changes in plateau volume were observed on subsequent follow-up, as previously seen.[17] In all eyes of our series, a drusenoid PED was noted to precede the appearance
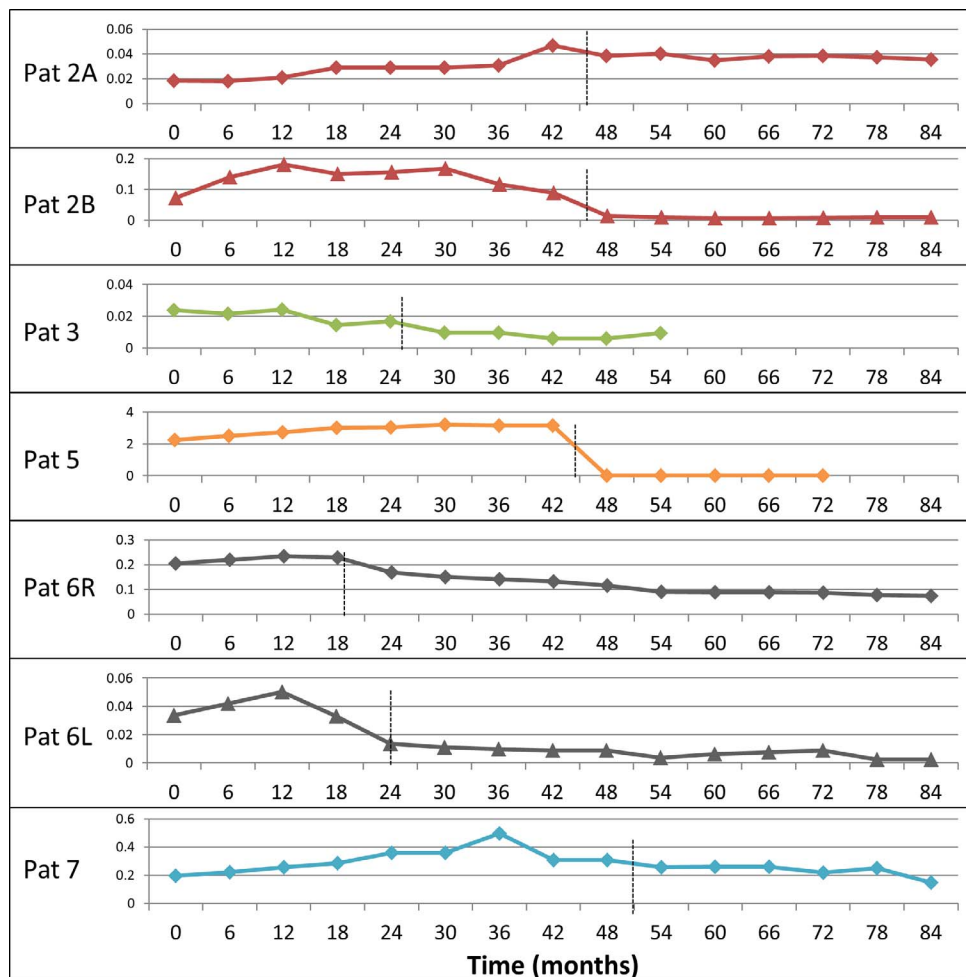
FIGURE 5. Volume (mm³) of PED measured in OCT over time. The point at which the plateaus form (complete loss of RPE from the hyperreflective RPE-BL complex over the PED) is shown by the *dotted line*. Patient 2 has two separate PEDs that evolve to two separate plateaus (**A**, **B**). Patient 6 has a plateau in both the right eye (R) and the left eye (L). Only patients with an intact hyperreflective RPE-BL complex baseline were included in this analysis. When the plateau signature is first observed (*black dotted line*), a decrease in the volume that stabilizes on further follow-up.

of the plateau. In a prior description, plateaus were thought to evolve in the outer retina and the hyperreflective line that is likely persistent BLamD was attributed to the OPL.[17] In contrast, serial eye-tracked OCT imaging in our cases shows that changes occurred in the sub-RPE compartment, defined in atrophic eyes as the space external to persistent BLamD.[38,39] During development of a plateau, its thin hyperreflective surface, having emerged after RPE atrophy, is readily distinguishable from the overlying subsiding OPL (Figs. 1, 2).

Plateaus are one route from drusenoid PED to atrophy, and they can be contrasted with a route via PED growth and collapse, which we recently described.[10] Growth and collapse of large PED appear to be on a continuum with similar changes described for smaller drusen.[10] Why a PED in any one eye proceeds to a plateau or to collapse is not known at present. Our detailed description of plateaus will facilitate mechanistic thinking and guide the design of future studies with more patients to investigate associated risk factors that may have prognostic value. Evolution of a plateau entails at least four processes that are discernible at the histologic level and also in SD-OCT. In approximately chronologic order, the sequence of the evolution is as follows: loss of RPE, persistence of BLamD, followed by concurrent clearing of druse contents and occupation of druse space by cellular processes. The loss of

RPE is the point at which a drusenoid PED becomes a plateau, and it is marked by a thick, roughened, and highly hyperreflective band becoming thinner, smoother, and moderately hyperreflective. Hyperreflective foci over PED destined for plateaus were noted in our series, suggestive of anterior RPE migration, as also seen over PED destined for collapse.[10] The development of GA is hypothesized to proceed via two main pathways of RPE fate,[29] including migration of fully pigmented and nucleated RPE into the retina (called "sloughed" and "intraretinal") and shedding of non-nucleated granule aggregates, possibly apoptotic remnants, into underlying BLamD. Our previous studies correlated intraretinal hyperreflective foci seen on in vivo and ex vivo OCT with anteriorly migrating RPE cells.[10,11,35] Thus, we have good reason to suspect that the spherical hyperreflective intraretinal foci directly internal to the plateaus are also migrating RPE cells.

The thin, moderately hyperreflective band draped over plateaus is persistent BLamD that maintains the shape of the original PED. BLamD is a stereotypically structured thick layer of basement membrane material that was initially used by Sarks et al.[34] to stage AMD eyes and has been recently shown to be clinically visible by SD-OCT.[14,40,41] A basement membrane is a defining feature of an epithelium, as is the RPE. BLamD is composed of basement membrane proteins and carbohydrate-
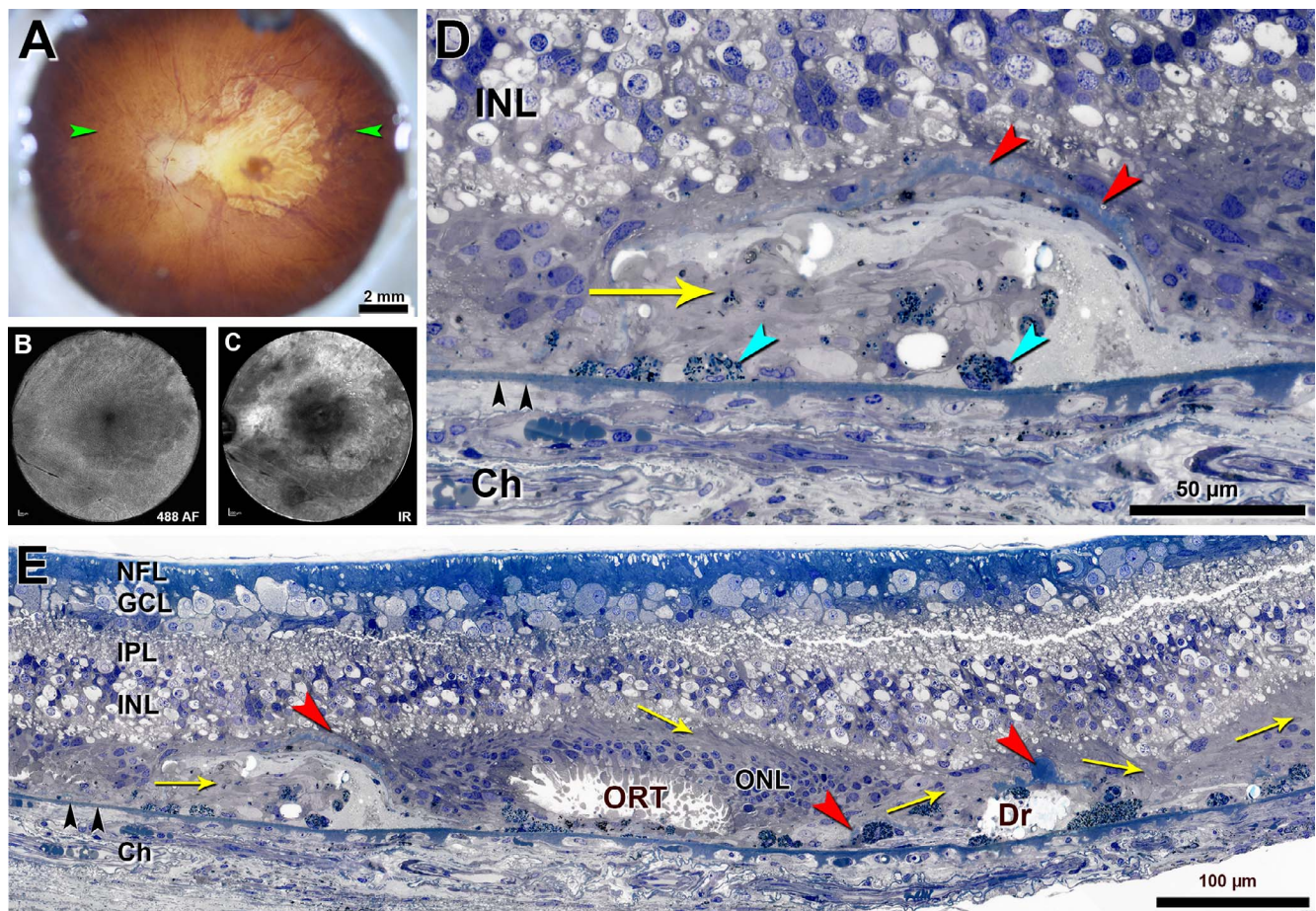
FIGURE 6. Persistent BL deposit and Müller cell processes in GA in a 95-year-old white man. Submicrometer epoxy section with toluidine blue stain. Tissue was postfixed in osmium tannic acid paraphenylenediamine. (**A–C**) Ex vivo imaging of postmortem fundus. (**A**) CFP (*top row left*) shows a large area of atrophy of RPE extending to the optic nerve head but sparing the fovea. Choroidal vessels emptied of blood are visible due to intervening stromal melanocytes. *Green arrowheads* approximate the level of the histologic section shown in the *top far right* and *bottom*. (**B**) Ex vivo 488-nm autofluorescence shows loss of signal in the atrophic area. (**C**) Ex vivo NIR imaging shows small and highly reflective puncta in the atrophic area. Detailed (**D**) and panoramic (**E**) views of the atrophic area in histology. *Red arrowheads*: BLamD. *Black arrowheads*: BrM. NFL, nerve fiber layer; GCL, ganglion cell layer; IPL, inner plexiform layer; Dr, calcified druse. (**D**) Processes from Müller cells under a corrugation of persistent BLamD in the atrophic area. This corrugation overlies "subducted" cells of RPE origin[29] (*teal arrowheads*), which contain nuclei, spindle-shaped melanosomes, and lipofuscin, and are located external to BLamD, on BrM. Müller cell processes appear to enter the corrugation horizontally from the left (*yellow arrow*) and sweep the pigmented cells away. (**E**) BLamD is discontinuous and present at three separate locations (*red arrows*). All visible pigmented cells are "subducted." In the normal Henle fiber layer, Müller cell processes are obliquely oriented (outer-center to inner-periphery), and they are parallel to, and interleaved with, inner fibers of cone and rod photoreceptors.[31] In the presence of severe photoreceptor degeneration, the trajectories of gliotic Müller cell processes and remaining photoreceptors are oriented in many directions (*yellow arrows*).

bearing moieties. It is crossed by lipoprotein particles en route to BrM and choriocapillaris for apparent egress to the systemic circulation.[42–44] BLamD observed on OCT is typically shadowed by the RPE. When BLamD is thick enough to be visible, it is observable as a hyporeflective layer.[14,40,41] After the RPE atrophies and can no longer cast a shadow, BLamD emerges as a moderately hyperreflective line of overall horizontal orientation that is sometimes corrugated. Outer retinal corrugations were proposed to be contraction folds of persistent BLamD created by loss of neovascular tissue or drusen/basal linear deposit previously located in the sub-RPE space.[14] Here we extend this model to large drusenoid PED, on the grounds that corrugations and plateaus represent a continuum of OCT signatures involving persistent BLamD. Further, we propose on the basis of prior pathology literature a possible mechanism for how sub-RPE material may be cleared and the shape of persistent BLamD established. Thus, our observations on a histologic case with an apparent corrugation (Fig. 6) can be cautiously extrapolated to a plateau, which is larger.

Our clinical series showed that most of the PEDs that evolved into plateaus were drusenoid, and druse contents (e.g., lipids, proteins, and minerals[24,45]) appear to be removed, replaced, or both, over time. The cells and secreted factors (e.g., metalloproteinases, lipases) responsible for druse removal are not established. Müller cells are candidates, because previous studies have shown that Müller cell processes may protrude into the sub-RPE space,[14,34] extend over BrM,[46,47] and break up persistent BLamD.[14,48] Müller cells are instrumental in forming ORT[13] and delimiting the border of photoreceptor atrophy.[39] Gliosis indicated by intense glial fibrillary acidic protein immunoreactivity is prominent in areas of severe photoreceptor loss and RPE atrophy,[46,47,49] and Müller cells remain when all photoreceptors have died.[13] In our exemplar histologic case, proteinaceous PED contents appear to be replaced by invading cellular processes (Fig. 6)[34] that are consistent with designation as Müller cells based on this literature. We hypothesize that plateau and corrugation formation requires extension of Müller cell processes through

defects in the RPE/BLamD complex (Figs. 4, 6) that occur during the life cycle of drusenoid PEDs. We further hypothesize that increasing hyporeflectivity observed within the sub-RPE space during the progression of drusenoid PEDs represents a change in composition of the sub-RPE material that encourages the entry of these processes.

The strength of this research is the long follow-up period for our patient cohort, with serial eye-tracked SD-OCT imaging for up to 7 years and notably dating back to before the development of GA in all but one eye. Another strength is the availability of up to nine separate imaging technologies, each specifically highlighting different tissue features in any one case and the availability of one illustrative histology case. Limitations include the small number of eyes and the absence of direct correlation of in vivo imaging to postmortem histology; hence, although our hypothesis of Müller cells involvement in plateau formation is credible and testable,[50] whether these cellular activities are directly visible in OCT is currently unknown. Our technique of volume measurement may be subject to variations according to OCT B-scan density between patients, but for our purpose of studying progression on a per-patient basis, this limitation was acceptable. To minimize inconsistencies, all patients in our study had eye-tracked scans at each follow-up visit with similar density scan patterns available for analysis.

Our study adds value to existing literature on PED by suggesting a role of Müller cell gliosis, elongation, and elaboration in the pathogenesis of AMD, which should be further explored in future studies. It is important for clinicians to be aware of plateaus and to distinguish them from OCT findings related to neovascular AMD, such as vascularized PEDs or signs of exudation, as OCTA imaging of three eyes in our study showed no evidence of neovascular flow within plateaus (Fig. 4). Plateau structures should not be confused with areas of subretinal fluid and treatment is not indicated for this finding. Finally, the distinctive reflectivity of persistent BLamD in outer retinal corrugations, and, now, plateaus, provides strong motivation for renaming the fourth outer retinal hyperreflective band of normal eyes, which is currently called the RPE-BrM complex,[23] to the RPE-BLam-BrM complex (abbreviated as RBB)[26] to accommodate the appearance of PED and persistent BLamD in eyes with AMD.

References

1. Wong WL, Su X, Li X, et al. Global prevalence of age-related macular degeneration and disease burden projection for 2020 and 2040: a systematic review and meta-analysis. *The Lancet Glob Health*. 2014;2:e106–e116.

2. Jonas JB, Bourne RR, White RA, et al. Visual impairment and blindness due to macular diseases globally: a systematic review and meta-analysis. *Am J Ophthalmol*. 2014;158:808–815.

3. Maguire MG, Martin DF, Ying GS, et al.; CATT Research Group. Five-year outcomes with anti-vascular endothelial growth factor treatment of neovascular age-related macular degeneration: the comparison of age-related macular degeneration treatments trials. *Ophthalmology*. 2016;123:1751–1761.

4. Zarbin MA, Casaroli-Marano RP, Rosenfeld PJ. Age-related macular degeneration: clinical findings, histopathology and imaging techniques. *Dev Ophthalmol*. 2014;53:1–32.

5. Schaal KB, Rosenfeld PJ, Gregori G, Yehoshua Z, Feuer WJ. Anatomic clinical trial endpoints for nonexudative age-related macular degeneration. *Ophthalmology*. 2016;123:1060–1079.

6. Wu Z, Luu CD, Ayton LN, et al. Optical coherence tomography-defined changes preceding the development of drusen-associated atrophy in age-related macular degeneration. *Ophthalmology*. 2014;121:2415–2422.

7. Schmitz-Valckenberg S, Fleckenstein M, Scholl HP, Holz FG. Fundus autofluorescence and progression of age-related macular degeneration. *Surv Ophthalmol*. 2009;54:96–117.

8. Cukras C, Agrón E, Klein ML, et al. Natural history of drusenoid pigment epithelial detachment in age-related macular degeneration: Age-Related Eye Disease Study Report No. 28. *Ophthalmology*. 2010;117:489–499.

9. Holz FG, Strauss EC, Schmitz-Valckenberg S, van Lookeren Campagne M. Geographic atrophy: clinical features and potential therapeutic approaches. *Ophthalmology*. 2014; 121:1079–1091.

10. Balaratnasingam C, Yannuzzi LA, Curcio CA, et al. Associations between retinal pigment epithelium and drusen volume changes during the lifecycle of large drusenoid pigment epithelial detachments. *Invest Ophthalmol Vis Sci*. 2016;57: 5479–5489.

11. Schlanitz FG, Baumann B, Kundi M, et al. Drusen volume development over time and its relevance to the course of age-related macular degeneration. *Br J Ophthalmol*. 2016;101: 198–203.

12. Ouyang Y, Heussen FM, Hariri A, Keane PA, Sadda SR. Optical coherence tomography-based observation of the natural history of drusenoid lesion in eyes with dry age-related macular degeneration. *Ophthalmology*. 2013;120:2656–2665.

13. Schaal KB, Freund KB, Litts KM, Zhang Y, Messinger JD, Curcio CA. Outer retinal tubulation in advanced age-related macular degeneration: optical coherence tomographic findings correspond to histology. *Retina*. 2015;35:1339–1350.

14. Ooto S, Vongkulsiri S, Sato T, Suzuki M, Curcio CA, Spaide RF. Outer retinal corrugations in age-related macular degeneration. *JAMA Ophthalmol*. 2014;132:806–813.

15. Fleckenstein M, Charbel Issa P, Helb HM, et al. High-resolution spectral domain-OCT imaging in geographic atrophy associated with age-related macular degeneration. *Invest Ophthalmol Vis Sci*. 2008;49:4137–4144.

16. Bonnet C, Querques G, Zerbib J, et al. Hyperreflective pyramidal structures on optical coherence tomography in geographic atrophy areas. *Retina*. 2014;34:1524–1530.

17. Querques G, Capuano V, Frascio P, Zweifel S, Georges A, Souied EH. Wedge-shaped subretinal hyporeflectivity in geographic atrophy. *Retina*. 2015;35:1735–1742.

18. Monés J, Biarnes M, Trindade F. Hyporeflective wedge-shaped band in geographic atrophy secondary to age-related macular degeneration: an underreported finding. *Ophthalmology*. 2012;119:1412–1419.

19. Querques G. Reply. *Retina*. 2016;36:e21–e22.

20. Monés J, Biarnes M. Correspondence. *Retina*. 2016;36:e20.

21. Suzuki M, Curcio CA, Mullins RF, Spaide RF. Refractile drusen: clinical imaging and candidate histology. *Retina*. 2015;35: 859–865.

22. Schindelin J, Arganda-Carreras I, Frise E, et al. Fiji: an open-source platform for biological-image analysis. *Nat Methods*. 2012;9:676–682.

23. Staurenghi G, Sadda S, Chakravarthy U, Spaide RF; International Nomenclature for Optical Coherence Tomography Panel. Proposed lexicon for anatomic landmarks in normal posterior segment spectral-domain optical coherence tomography: the IN*OCT consensus. *Ophthalmology*. 2014;121: 1572–1578.

24. Curcio CA, Johnson M. *Structure, Function, and Pathology of Bruch's Membrane*. London: Elsevier; 2013.

25. Prakash YS, Smithson KG, Sieck GC. Application of the Cavalieri principle in volume estimation using laser confocal microscopy. *NeuroImage*. 1994;1:325–333.

26. Balaratnasingam C, Hoang QV, Inoue M, et al. Clinical characteristics, choroidal neovascularization and predictors of visual outcomes in acquired vitelliform lesions. *Am J Ophthalmol*. 2016;172:28–38.

27. Pang C, Messinger JD, Zanzottera EC, Freund KB, Curcio CA. The Onion Sign in neovascular age-related macular degeneration represents cholesterol crystals. *Ophthalmology*. 2015; 122:2316–2326.

28. Curcio CA, Messinger JD, Mitra AM, Sloan KR, McGwin G Jr, Spaide R. Human chorioretinal layer thicknesses measured using macula-wide high resolution histological sections. *Invest Ophthalmol Vis Sci*. 2011;52:3943–3954.

29. Zanzottera EC, Messinger JD, Ach T, Smith RT, Curcio CA. Subducted and melanotic cells in advanced age-related macular degeneration are derived from retinal pigment epithelium. *Invest Ophthalmol Vis Sci*. 2015;56:3269–3278.

30. Polyak S. *The Vertebrate Visual System*. Chicago: The University of Chicago Press; 1957.

31. Perry VH, Cowey A. The lengths of the fibres of Henle in the retina of macaque monkeys: implications for vision. *Neuroscience*. 1988;25:225–236.

32. Gass JD. Drusen and disciform macular detachment and degeneration. *Trans Am Ophthalmol Soc*. 1972;70:409–436.

33. Klein ML, Ferris FL III, Armstrong J, et al. Retinal precursors and the development of geographic atrophy in age-related macular degeneration. *Ophthalmology*. 2008;115:1026–1031.

34. Sarks JP, Sarks SH, Killingsworth MC. Evolution of geographic atrophy of the retinal pigment epithelium. *Eye*. 1988;2:552–577.

35. Zanzottera EC, Messinger JD, Ach T, Smith RT, Freund KB, Curcio CA. The Project MACULA retinal pigment epithelium grading system for histology and optical coherence tomography in age-related macular degeneration. *Invest Ophthalmol Vis Sci*. 2015;56:3253–3268.

36. Gocho K, Sarda V, Falah S, et al. Adaptive optics imaging of geographic atrophy. *Invest Ophthalmol Vis Sci*. 2013;54: 3673–3680.

37. Balaratnasingam C, Messinger JD, Sloan KR, Yannuzzi LA, Freund KB, Curcio CA. Histologic and optical coherence tomographic correlates in drusenoid pigment epithelium detachment in age-related macular degeneration [published online ahead of print January 30, 2017]. *Ophthalmology*. doi: 10.1016/j.ophtha.2016.12.034.

38. Green WR, Enger C. Age-related macular degeneration histopathologic studies. The 1992 Lorenz E. Zimmerman Lecture. *Ophthalmology*. 1993;100:1519–1535.

39. Zanzottera EC, Ach T, Huisingh C, Messinger JD, Freund KB, Curcio CA. Visualizing retinal pigment epithelium phenotypes in the transition to atrophy in neovascular age-related macular degeneration. *Retina*. 2016;36:S26–S39.

40. Fleckenstein M, Schmitz-Valckenberg S, Martens C, et al. Fundus autofluorescence and spectral-domain optical coherence tomography characteristics in a rapidly progressing form of geographic atrophy. *Invest Ophthalmol Vis Sci*. 2011;52: 3761–3766.

41. Curcio CA, Balaratnasingam C, Messinger JD, Yannuzzi LA, Freund KB. Correlation of type 1 neovascularization associated with acquired vitelliform lesion in the setting of age-related macular degeneration. *Am J Ophthalmol*. 2015;160: 1024–1033.

42. Holz FG, Sheraidah G, Pauleikhoff D, Bird AC. Analysis of lipid deposits extracted from human macular and peripheral Bruch's membrane. *Arch Ophthalmol*. 1994;112:402–406.

43. Kliffen M, Mooy CM, Luider TM, Huijmans JG, Kerkvliet S, de Jong PT. Identification of glycosaminoglycans in age-related macular deposits. *Arch Ophthalmol*. 1996;114:1009–1014.

44. Pauleikhoff D, Sheraidah G, Marshall J, Bird AC, Wessing A. Biochemical and histochemical analysis of age related lipid deposits in Bruch's membrane [in German]. *Ophthalmologe*. 1994;91:730–734.

45. Curcio CA, Millican CL. Basal linear deposit and large drusen are specific for early age-related maculopathy. *Arch Ophthalmol*. 1999;117:329–339.

46. Guidry C, Medeiros NE, Curcio CA. Phenotypic variation of retinal pigment epithelium in age-related macular degeneration. *Invest Ophthalmol Vis Sci*. 2002;43:267–273.

47. Wu KH, Madigan MC, Billson FA, Penfold PL. Differential expression of GFAP in early v late AMD: a quantitative analysis. *Br J Ophthalmol*. 2003;87:1159–1166.

48. Gupta N, Brown KE, Milam AH. Activated microglia in human retinitis pigmentosa, late-onset retinal degeneration, and age-related macular degeneration. *Exp Eye Res*. 2003;76:463–471.

49. Johnson PT, Lewis GP, Talaga KC, et al. Drusen-associated degeneration in the retina. *Invest Ophthalmol Vis Sci*. 2003; 44:4481–4488.

50. Hippert C, Graca AB, Barber AC, et al. Müller glia activation in response to inherited retinal degeneration is highly varied and disease-specific. *PLoS One*. 2015;10:e0120415.